9
Partons

Equipped with the formalism of Chapter 8, we can now turn to the experimental information and ask the question, "Can small-wavelength photons resolve the quarks inside the proton target?"

9.1 Bjorken Scaling

If simple, point-like, spin-$\frac{1}{2}$ quarks reside inside the proton, we should be able to illuminate them with a small-wavelength (large $-q^2$) virtual photon beam (Fig. 9.1). The fact that such photons break up the proton target can be handled by using the inelastic form factors discussed in the previous chapter. The sign that there are structureless particles inside a complex system like a proton is that for small wavelengths, the proton described by (8.43) suddenly starts behaving like a free Dirac particle (a quark) and (8.43) turns into (8.41). The proton structure functions thus become simply

$$2W_1^{\text{point}} = \frac{Q^2}{2m^2}\delta\left(\nu - \frac{Q^2}{2m}\right),$$
$$W_2^{\text{point}} = \delta\left(\nu - \frac{Q^2}{2m}\right). \tag{9.1}$$

For convenience, we have introduced the positive variable

$$Q^2 \equiv -q^2.$$

Here, m is the quark mass; the "point" notation reminds us the quark is a structureless Dirac particle. Equation (9.1) can be pictured as

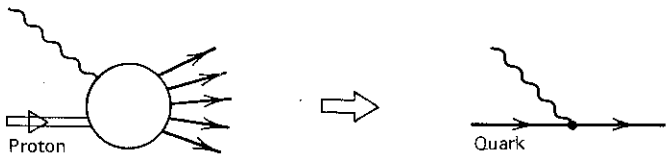

(9.2)

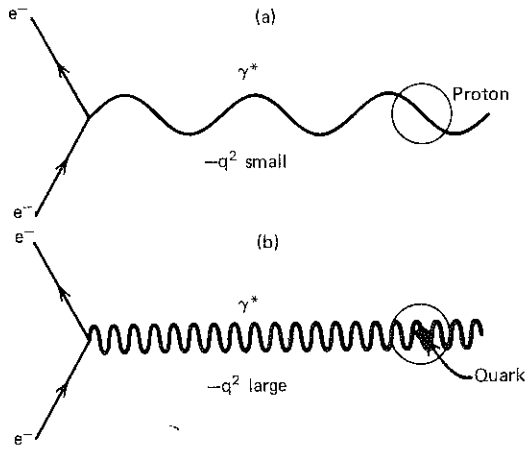

Fig. 9.1 (a) Elastic ep → ep scattering in which a large-wavelength "photon beam" measures the size of the proton through the elastic form factor analysis. (b) In deep inelastic scattering a short-wavelength "photon beam" resolves the quarks within the proton provided $\lambda\left(\approx 1/\sqrt{-q^2}\right) \ll 1\text{F}$.

that is, at large Q^2, *inelastic* electron–proton scattering is viewed simply as *elastic* scattering of the electron on a "free" quark within the proton. Using the identity $\delta(x/a) = a\,\delta(x)$, (9.1) may be rearranged to introduce dimensionless structure functions

$$2mW_1^{\text{point}}(\nu, Q^2) = \frac{Q^2}{2m\nu}\delta\left(1 - \frac{Q^2}{2m\nu}\right),$$
$$\nu W_2^{\text{point}}(\nu, Q^2) = \delta\left(1 - \frac{Q^2}{2m\nu}\right). \tag{9.3}$$

These "point" functions now display the intriguing property that they are only functions of the ratio $Q^2/2m\nu$ and *not* of Q^2 and ν independently. This behavior can be contrasted with that for ep elastic scattering. For simplicity, set $\kappa = 0$, so that $G_E = G_M \equiv G$; then, comparing (8.42) and (8.43), we have

$$W_1^{\text{elastic}} = \frac{Q^2}{4M^2}G^2(Q^2)\delta\left(\nu - \frac{Q^2}{2M}\right),$$
$$W_2^{\text{elastic}} = G^2(Q^2)\delta\left(\nu - \frac{Q^2}{2M}\right). \tag{9.4}$$

In contrast to (9.1), the structure functions of (9.4) contain a form factor $G(Q^2)$, and so cannot be rearranged to be functions of a single dimensionless variable. A

mass scale is explicitly present; it is set by the empirical value 0.71 GeV in the dipole formula for $G(Q^2)$ which reflects the inverse size of the proton, see (8.20). As Q^2 increases above $(0.71\ \text{GeV})^2$, the form factor depresses the chance of elastic scattering; the proton is more likely to break up. The point structure functions, on the other hand, depend only on a dimensionless variable $Q^2/2m\nu$, and no scale of mass is present. The mass m merely serves as a scale for the momenta Q^2, ν.

The discussion can be summarized as follows: if large Q^2 virtual photons resolve "point" constituents inside the proton, then

$$MW_1(\nu, Q^2) \underset{\text{large } Q^2}{\longrightarrow} F_1(\omega),$$
$$\nu W_2(\nu, Q^2) \underset{\text{large } Q^2}{\longrightarrow} F_2(\omega), \tag{9.5}$$

where

$$\omega = \frac{2q \cdot p}{Q^2} = \frac{2M\nu}{Q^2}. \tag{9.6}$$

Note that in (9.5) we have changed the scale from what it was in (9.3). We have introduced the proton mass instead of the quark mass to define the dimensionless variable ω. The presence of free quarks is signaled by the fact that the inelastic structure functions are independent of Q^2 at a given value of ω [see (9.5)]. This is equivalent to the onset of $\sin^{-4}(\theta/2)$ behavior for large momentum transfers in the Rutherford experiment, which reveals the "point" charge of the nucleus in the atom. A sample of data is shown in Fig. 9.2. νW_2 at $\omega = 4$ is independent of Q^2; the photon is indeed interacting with point-like particles. No form factors, leading to additional Q^2 dependence as in (9.4), are present. Are these particles (called partons by Bjorken) the same as the quarks discovered in the spectroscopy of hadrons (Chapter 2)?

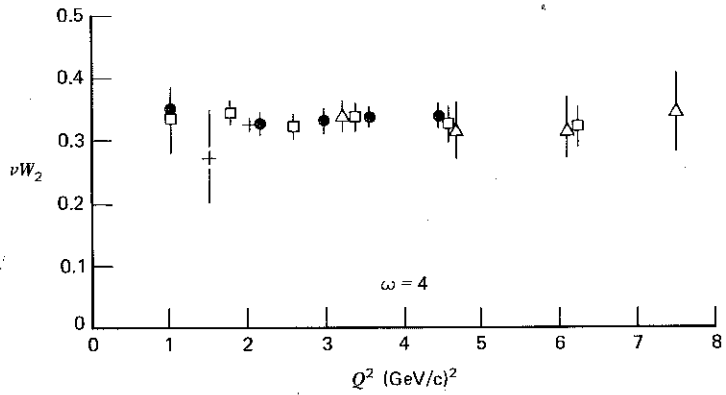

Fig. 9.2 The structure function νW_2 determined by electron–proton scattering as a function of Q^2 for $\omega = 4$. Data are from the Stanford Linear Accelerator.

9.2 Partons and Bjorken Scaling

Now that scaling is an approximate experimental fact, we attempt to make the identification of (9.2) explicit:

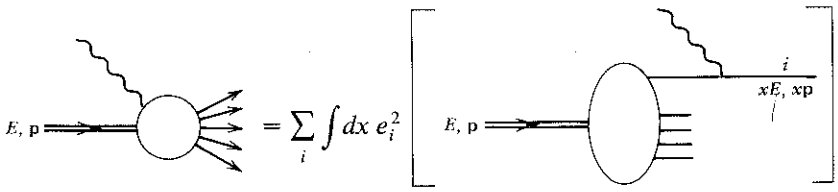

(9.7)

Equation (9.7) recognizes the fact that various types of "point" partons make up the proton (i = u, d, . . . , quarks, with various charges e_i, as well as gluons; the latter do not interact with the photon, of course). They can each carry a different fraction x of the parent proton's momentum and energy. We introduce the parton momentum distribution

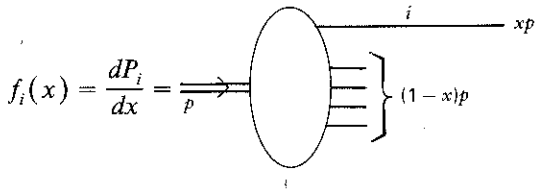

(9.8)

which describes the probability that the struck parton i carries a fraction x of the proton's momentum p. All the fractions x have to add up to 1; therefore,

$$\sum_{i'} \int dx\, x f_{i'}(x) = 1. \tag{9.9}$$

Here, i' sums over all the partons, not just the charged ones i which interact with the photon. The kinematics can be summarized as follows:

	Proton ↓	Parton ↓
Energy	E	xE
Momentum	p_L	xp_L
	$p_T = 0$	$p_T = 0$
Mass	M	$m = (x^2E^2 - x^2p_L^2)^{1/2} = xM.$

(9.10)

Both the proton and its parton progeny move along the z axis (i.e., $p_T = 0$) with longitudinal momenta p_L and xp_L. The definition of the reference frame has to be made with more care; we shall return to it later on.

For an electron hitting a parton with momentum fraction x and unit charge, we see from (9.3) and (9.5) that the dimensionless structure functions are

$$F_1(\omega) = \frac{Q^2}{4m\nu x}\delta\left(1 - \frac{Q^2}{2m\nu}\right) = \frac{1}{2x^2\omega}\delta\left(1 - \frac{1}{x\omega}\right),$$

$$F_2(\omega) = \delta\left(1 - \frac{Q^2}{2m\nu}\right) = \delta\left(1 - \frac{1}{x\omega}\right). \tag{9.11}$$

We have used the kinematics of (9.10); ω is the dimensionless variable defined in (9.6). Summing our results for $F_{1,2}$ for one parton, (9.11), over the partons making up a proton, (9.7) and (9.8), we obtain

$$F_2(\omega) = \sum_i \int dx\, e_i^2 f_i(x) x\, \delta\left(x - \frac{1}{\omega}\right),$$

$$F_1(\omega) = \frac{\omega}{2} F_2(\omega). \tag{9.12}$$

It is conventional to redefine $F_{1,2}(\omega)$ as $F_{1,2}(x)$ and to express the results in terms of x. Recalling the identification (9.5), we see that (9.12) become, at large Q^2,

$$\boxed{\nu W_2(\nu, Q^2) \to F_2(x) = \sum_i e_i^2 x f_i(x),} \tag{9.13}$$

$$\boxed{MW_1(\nu, Q^2) \to F_1(x) = \frac{1}{2x} F_2(x),} \tag{9.14}$$

with

$$x = \frac{1}{\omega} = \frac{Q^2}{2M\nu}. \tag{9.15}$$

That is, the momentum fraction is found to be identical to the (dimensionless) kinematic variable x of the virtual photon that we introduced in Chapter 8; see (8.30). In other words, the virtual photon must have just the right value of the variable x to be absorbed by a parton with momentum fraction x. It is the delta function in (9.12) that equates these two distinct physical variables.

The inelastic structure functions $F_{1,2}$ of (9.13) and (9.14) are functions of only one variable, namely, x. They are independent of Q^2 at fixed x. We say they satisfy Bjorken scaling.

EXERCISE 9.1 Prove that $0 \le x \le 1$, as it must be if x represents a momentum fraction; recall Exercise 8.11.

Note that the kinematics, (9.10), are a bit funny. Assigning a variable mass xM to the parton is of course out of the question. Clearly, if the parton's momentum

is xp, its energy can only be xE if we put $m = M = 0$. Equivalently, a proton can only emit a parton moving parallel to it ($p_T = 0$ for both) if they both have zero mass. A corollary to this statement is that if a massive particle decays, there is a nonzero angle between its decay products. We justify our previous calculation by working in a Lorentz frame where

$$|\mathbf{p}| \gg m, M, \tag{9.16}$$

so that all masses can be neglected. In this frame, where the proton is moving with infinite momentum, the kinematics of (9.10) and the structure of $F_{1,2}(x)$ given by (9.13) and (9.14) become exact. In this frame, relativistic time dilation slows down the rate at which partons interact with one another; that is, during the short time the virtual photon interacts with the quark [see (9.7)], it is essentially a free particle, not interacting with its friends in the proton. We implicitly used this *incoherence* assumption in the derivation of $F_{1,2}(x)$; (9.7) represents an addition of probabilities (not amplitudes) of scattering from *single* free partons. It is the analogue of the impulse approximation in nuclear physics. However, there is a difference. A struck nucleon can escape from the nucleus as a completely free particle, but the struck colored parton has to recombine with the noninteracting spectator partons to form the colorless hadrons into which the proton breaks up. This has to happen with probability 1, because of color confinement (see Chapter 1); and, due to the size of the proton, it requires a much longer time scale than the quick punch the parton receives from the virtual photon. In summary, we argue that in a hard collision, the parton recoils as if it were free enabling the ep → eX cross section to be calculated [see (8.43), (9.13), and (9.14)] and that the subsequent confining final state interactions do not affect the result. This picture is valid when both the Q^2 of the virtual photon and the invariant mass of the final-state hadronic system, W, are large.

EXERCISE 9.2 Convince yourself that the interaction time is much shorter than the time scale over which the partons inside the target interact with one another. Read the explicit derivation in J. D. Bjorken and E. A. Paschos, *Phys. Rev. 185*, 1975 (1969); see also Perl (1974).

EXERCISE 9.3 It is helpful to work through an alternative derivation of the parton model result, (9.13)–(9.15), in terms of the invariant variables of (6.29):

$$s \simeq 2k \cdot p, \qquad u \simeq -2k' \cdot p, \qquad t \equiv -Q^2 = -2k \cdot k',$$

with particle masses neglected. Set the parton momentum $\hat{p} = xp$, that is, neglect its component transverse to the proton momentum p. We outline the steps below. Using the basic idea of (9.7), we can write

$$\left(\frac{d\sigma}{dt\,du}\right)_{\mathrm{ep}\to\mathrm{eX}} = \sum_i \int dx\, f_i(x) \left(\frac{d\sigma}{dt\,du}\right)_{\mathrm{eq}_i\to\mathrm{eq}_i}, \tag{9.17}$$

that is, the ep → eX rate is simply the incoherent sum over all the contributing partons. Show that the invariant variables for the parton subprocess are given by

$$\hat{s} = xs, \qquad \hat{u} = xu, \qquad \hat{t} = t.$$

Use these relations, together with the eμ scattering amplitude of (6.30), to show that

$$\left(\frac{d\sigma}{dt\,du}\right)_{\mathrm{eq}_i \to \mathrm{eq}_i} = x\frac{d\sigma}{d\hat{t}\,d\hat{u}} = x\frac{2\pi\alpha^2 e_i^2}{t^2}\left(\frac{s^2+u^2}{s^2}\right)\delta(t + x(s+u)). \tag{9.18}$$

Now, also express the left-hand side of (9.17) in terms of s, t, and u. It is simplest to use (8.31). Verify that

$$\left(\frac{d\sigma}{dt\,du}\right)_{\mathrm{ep}\to\mathrm{eX}} = \frac{4\pi\alpha^2}{t^2 s^2}\frac{1}{s+u}\left[(s+u)^2 xF_1 - usF_2\right], \tag{9.19}$$

where $F_1 \equiv MW_1$ and $F_2 \equiv \nu W_2$. Insert (9.18) and (9.19) into (9.17). Compare coefficients of us and $s^2 + u^2$ and so obtain the master formula of the parton model:

$$\boxed{2x\,F_1(x) = F_2(x) = \sum_i e_i^2 x\,f_i(x).}$$

As before, we see that $F_{1,2}$ are functions only of the scaling variable x, here fixed by the delta function in (9.18):

$$x = \frac{-t}{s+u} = \frac{Q^2}{2M\nu}. \tag{9.20}$$

EXERCISE 9.4 In Chapter 8, we evaluated the ep → eX cross section for the electron to be scattered into the $dE'\,d\Omega$ element in the target proton rest frame (the laboratory frame). Show that

$$dE'\,d\Omega = \frac{\pi}{EE'}dQ^2\,d\nu = \frac{2ME}{E'}\pi y\,dx\,dy, \tag{9.21}$$

where x and y are the dimensionless variables

$$x = \frac{Q^2}{2M\nu}, \qquad y = \frac{p\cdot q}{p\cdot k}\underset{\text{(lab.)}}{=}\frac{\nu}{E}, \tag{9.22}$$

see (8.30). The allowed kinematic region ($0 \le x, y \le 1$) is shown in Fig. 9.3.

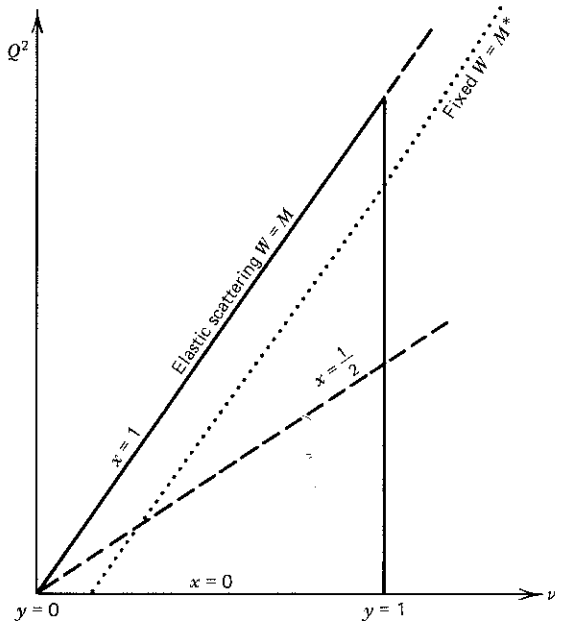

Fig. 9.3 The triangle is the allowed kinematic region for ep → eX. $\nu_{\max} = E$ in the laboratory frame. W is the invariant mass of the hadronic state X, see (8.29).

Verify that the ep → eX cross section may be written in the invariant form

$$M\nu_{\max}\frac{d\sigma}{dx\,dy} = \frac{2\pi\alpha^2}{x^2y^2}\left\{xy^2F_1 + \left[(1-y) - \frac{Mxy}{2\nu_{\max}}\right]F_2\right\}, \tag{9.23}$$

where $\nu_{\max} = E$ in the laboratory frame.

EXERCISE 9.5 Use (9.23) to show that the parton model predicts

$$\left(\frac{d\sigma}{dx\,dy}\right)_{ep\to eX} = \frac{2\pi\alpha^2}{Q^4}s\left[1+(1-y)^2\right]\sum_i e_i^2 x\, f_i(x) \tag{9.24}$$

if particle masses are neglected.

EXERCISE 9.6 Show that

$$1 - y = \frac{p\cdot k'}{p\cdot k} \simeq \frac{1}{2}(1+\cos\theta), \tag{9.25}$$

where θ is the scattering angle in the electron–quark center-of-mass frame.

Hence, identify the $(1-y)^2$ and 1 terms in (9.24) with scattering between an electron and quark with opposite helicities and with the same helicity, respectively.

The parton model result $2xF_1 = F_2$ is known as the Callan–Gross relation. It is a consequence of the quarks having spin $\frac{1}{2}$ and is well borne out by the data.

EXERCISE 9.7 In the limit ν, $Q^2 \to \infty$, with x fixed, show that the Callan–Gross relation implies that the virtual photon–quark cross sections of (8.53), (8.54) satisfy

$$\frac{\sigma_L}{\sigma_T} \to 0. \tag{9.26}$$

EXERCISE 9.8 Starting from (6.51), show that if quarks had spin 0, $F_2(x)$ would still be given by (9.13) but that $F_1(x) = 0$ and hence $\sigma_T = 0$.

Thus, in contrast to (9.26), spin-0 quarks would yield $\sigma_T/\sigma_L = 0$. We can understand this difference by glancing at Fig. 9.4, which shows the head-on collision between the quark and the virtual photon. By conservation of J_z (with z along **p**), we see that a spin-0 quark cannot absorb a photon of helicity $\lambda = \pm 1$, so $\sigma_T = 0$. Suppose now the quark has spin $\frac{1}{2}$. We recall that its helicity is conserved in a high-energy interaction (see Section 6.6). This can only be achieved by a $\lambda = \pm 1$ photon; hence, $\sigma_L \not\to 0$ in this case.

9.3 The Quarks Within the Proton

Does the photon see the proton structure described in Chapter 1, that is, does virtual photon–proton scattering look like Fig. 9.5? Just as measurements of elastic form factors provided us with information on the size of the proton, measurements on the inelastic structure function at large Q^2 reveal the quark structure of the proton. After establishing Bjorken scaling, telling us that the constituents are there, eqs. (9.13) and (9.14) become the tools for extracting further information. The sum in (9.13) runs over the charged partons in the

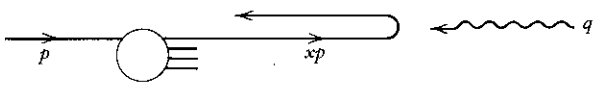

Fig. 9.4 Head-on collision between a constituent quark and the virtual photon.

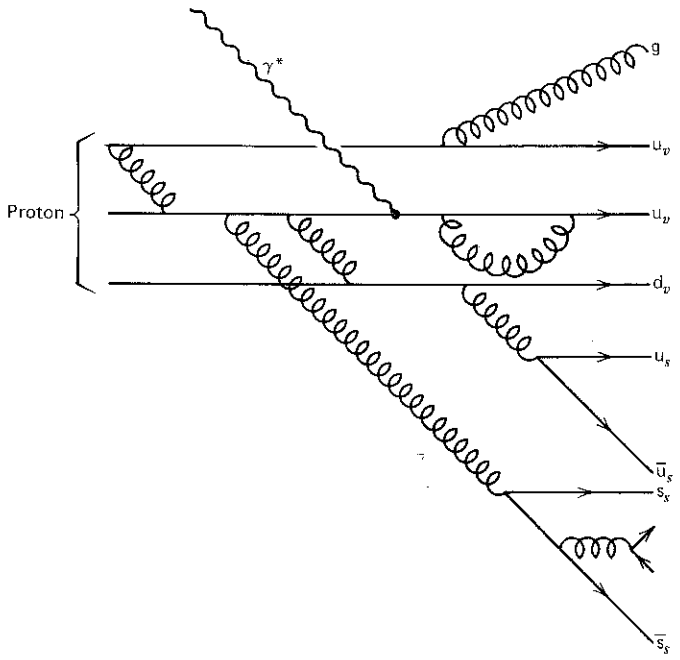

Fig. 9.5 A proton made up of valence quarks, gluons, and slow debris consisting of quark–antiquark pairs.

oton:

$$\frac{1}{x}F_2^{ep}(x) = \left(\frac{2}{3}\right)^2\left[u^p(x) + \bar{u}^p(x)\right] + \left(\frac{1}{3}\right)^2\left[d^p(x) + \bar{d}^p(x)\right] + \left(\frac{1}{3}\right)^2\left[s^p(x) + \bar{s}^p(x)\right], \tag{9.27}$$

here $u^p(x)$ and $\bar{u}^p(x)$ are the probability distributions of u quarks and ntiquarks within the proton. We have neglected the possibility of a sizable esence of charm and heavier quarks inside the proton.

We have six unknown quark structure functions, $f_i(x)$. However, the inelastic ructure functions for neutrons are experimentally accessible by scattering elec- ons from a deuterium target. The counterpart to (9.27) is

$$\frac{1}{x}F_2^{en} = \left(\frac{2}{3}\right)^2\left[u^n + \bar{u}^n\right] + \left(\frac{1}{3}\right)^2\left[d^n + \bar{d}^n\right] + \left(\frac{1}{3}\right)^2\left[s^n + \bar{s}^n\right]; \tag{9.28}$$

d as the proton and neutron are members of an isospin doublet, their quark ntent is related. There are as many u quarks in a proton as d quarks in a

neutron, and so on. So

$$\begin{aligned} u^p(x) &= d^n(x) \equiv u(x), \\ d^p(x) &= u^n(x) \equiv d(x), \\ s^p(x) &= s^n(x) \equiv s(x). \end{aligned} \tag{9.29}$$

EXERCISE 9.9 Show that the above expressions lead to the bounds

$$\frac{1}{4} \leq \frac{F_2^{en}(x)}{F_2^{ep}(x)} \leq 4$$

whatever the value of x. The lower (upper) limit would be realized if only u (d) quarks were present in the proton.

Further constraints on the quark structure functions $f_i(x)$ result from the fact that the quantum numbers of the proton must be exactly those of the uud combination of "valence" quarks of Chapter 2. As shown in Fig. 9.5, we describe the proton as three-constituent or three-valence quarks $u_v u_v d_v$ accompanied by many quark–antiquark pairs $u_s\bar{u}_s$, $d_s\bar{d}_s$, $s_s\bar{s}_s$, and so on. These are known as "sea" quarks. If we picture them as being radiated by the valence quarks, as in Fig. 9.5, then as a first approximation we may assume that the three lightest flavor quarks (u, d, s) occur in the "sea" with roughly the same frequency and momentum distribution, and neglect the heavier flavor quark pairs $c_s\bar{c}_s$, and so on. This picture of the proton can then be summarized as follows:

$$u_s(x) = \bar{u}_s(x) = d_s(x) = \bar{d}_s(x) = s_s(x) = \bar{s}_s(x) = S(x), \tag{9.30a}$$

$$u(x) = u_v(x) + u_s(x), \tag{9.30b}$$

$$d(x) = d_v(x) + d_s(x), \tag{9.30c}$$

where $S(x)$ is the sea quark distribution common to all quark flavors. Clearly, the heavier strange quarks are penalized in the radiation process by some threshold suppression so that (9.30a) is only approximately true.

By summing over all contributing partons, we must recover the quantum numbers of the proton: charge 1, baryon number 1, strangeness 0. It follows that

$$\begin{aligned} \int_0^1 [u(x) - \bar{u}(x)]\, dx &= 2, \\ \int_0^1 [d(x) - \bar{d}(x)]\, dx &= 1, \\ \int_0^1 [s(x) - \bar{s}(x)]\, dx &= 0. \end{aligned} \tag{9.31}$$

These sum rules express the requirement that the net number of each kind of valence quark corresponds to the uud combination of constituents discussed in

$$d^n(x) \equiv u(x),$$
$$u^n(x) \equiv d(x), \qquad (9.$$
$$s^n(x) \equiv s(x).$$

ıbove expressions lead to the bounds

$$\frac{F_2^{en}(x)}{F_2^{ep}(x)} \leq 4$$

r (upper) limit would be realized if only u
ɔton.

ɜtructure functions $f_i(x)$ result from the f
proton must be exactly those of the u
Chapter 2. As shown in Fig. 9.5, we descr
ıree-valence quarks $u_v u_v d_v$ accompanied
$d_s\bar{d}_s$, $s_s\bar{s}_s$, and so on. These are known
being radiated by the valence quarks, as
ı we may assume that the three lightest fla
ith roughly the same frequency and mom
avier flavor quark pairs $c_s\bar{c}_s$, and so on. T
mmarized as follows:

$$= \bar{d}_s(x) = s_s(x) = \bar{s}_s(x) = S(x), \qquad (9.3$$

(9.3

(9.3

ion common to all quark flavors. Clearly,
l in the radiation process by some thresh
ɒproximately true.
ıg partons, we must recover the quant
ryon number 1, strangeness 0. It follows t

$$- \bar{u}(x)]\, dx = 2,$$

$$- \bar{d}(x)]\, dx = 1, \qquad (9.$$

$$- \bar{s}(x)]\, dx = 0.$$

ɜment that the net number of each kind
ud combination of constituents discussed

apter 2. Equation (9.31) clearly follows from (9.30) with

$$u - \bar{u} = u - \bar{u}_s = u - u_s = u_v,$$
$$d - \bar{d} = d - \bar{d}_s = d - d_s = d_v,$$
$$s - \bar{s} = s_s - \bar{s}_s = 0.$$

ɔte however that the sum rules are true in any picture where the sea is taken to made of quark–antiquark pairs, and so does not affect the quantum numbers the proton, which are exclusively determined by the valence quarks, as pressed by (9.31).

Combining (9.30) with (9.27) and (9.28), we obtain

$$\frac{1}{x}F_2^{ep} = \frac{1}{9}[4u_v + d_v] + \frac{4}{3}S,$$
$$\frac{1}{x}F_2^{en} = \frac{1}{9}[u_v + 4d_v] + \frac{4}{3}S, \qquad (9.32)$$

ere $\frac{4}{3}$ is the sum of e_i^2 over the six sea quark distributions. Since gluons create $q\bar{q}$ pairs in the sea, we expect $S(x)$ to have a bremsstrahlung-like spectrum at all x, so that the number of sea quarks grows logarithmically as $x \to 0$ (see ercise 9.10).

EXERCISE 9.10 Assume that the virtual photon–proton total cross section of Section 8.5 behaves like a constant as $x \to 0$, $\nu \to \infty$ for fixed Q^2, and hence show that

$$f_i(x) \xrightarrow[x\to 0]{} \frac{1}{x}. \qquad (9.33)$$

Thus, we have a logarithmic growth of partons at small x.

When probing the small-momentum ($x \approx 0$) debris of the proton, we therefore ticipate that the presence of the three valence quarks will be overshadowed by ese multiple, low-momentum $q\bar{q}$ pairs that make up the sea $S(x)$. According to 32), this means that

$$\frac{F_2^{en}(x)}{F_2^{ep}(x)} \xrightarrow[x\to 0]{} 1. \qquad (9.34)$$

ıis is indeed the case experimentally, as can be checked from the data in Fig. 5. On the other hand, when probing the large-momentum part of the proton ucture ($x \approx 1$), the fast-valence quarks u_v, d_v leave little momentum unoccpied for sea pairs. In this limit, the valence quarks dominate in (9.32), and erefore

$$\frac{F_2^{en}(x)}{F_2^{ep}(x)} \xrightarrow[x\to 1]{} \frac{u_v + 4d_v}{4u_v + d_v}. \qquad (9.35)$$

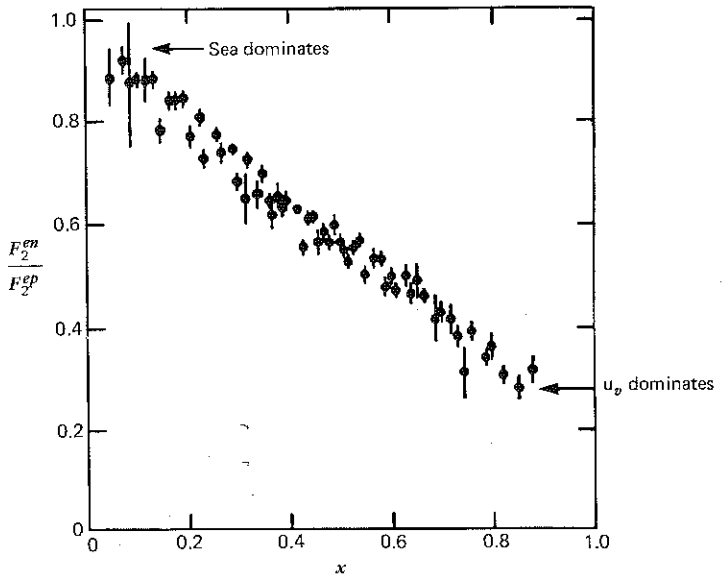

Fig. 9.6 The ratio F_2^{en}/F_2^{ep} as a function of x, measured in deep inelastic scattering. Data are from the Stanford Linear Accelerator.

For the proton, there is evidence that $u_v \gg d_v$ at large x, and the ratio (9.35) tends to $\frac{1}{4}$, as hinted at in Fig. 9.6.

EXERCISE 9.11 Discuss, on physical grounds, the behavior of $f_i(x)$ in the limit as $x \to 1$ when parton i carries all the momentum of the proton. Counting rules have been proposed which argue that

$$f_i(x) \underset{x \to 1}{\longrightarrow} (1-x)^{2n_s-1},$$

where n_s is the number of spectator valence quarks which share between them the residual, vanishingly small momentum of the proton. Contrast the $x \to 1$ behavior of $u^p(x)$ with that of $u^\pi(x)$, the u-quark structure function of a π^+-meson.

What should the complete $F_2(x)$ look like according to our picture of the proton (Fig. 9.5)? Its shape can be guessed by successive approximation; see Fig. 9.7. Figure 9.7 is self-explanatory. The transition from scenario 2 to 3 is of course due to the fact that once the quarks interact, they can redistribute the momenta among themselves, and the sharply defined momentum $x = \frac{1}{3}$ is washed out, becoming a distribution of momenta peaked around $x = \frac{1}{3}$. Data on $F_2^{ep}(x)$ at large Q^2 do indeed have the general shape of scenario 4 corresponding to Fig. 9.5.

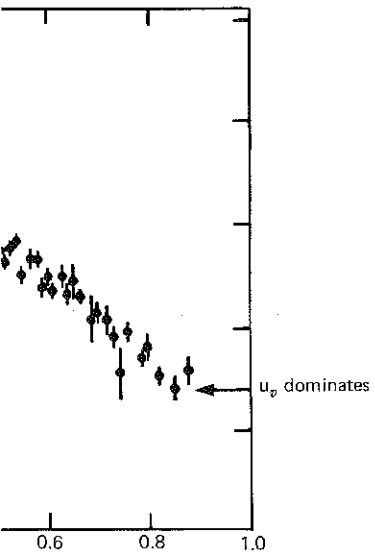

a function of x, measured in deep
n the Stanford Linear Accelerator.

$u_v \gg d_v$ at large x, and the ratio (9.35)

sical grounds, the behavior of $f_i(x)$ in
urries all the momentum of the proton.
which argue that

$$(1-x)^{2n_s-1},$$

r valence quarks which share between
momentum of the proton. Contrast the
of $u^\pi(x)$, the u-quark structure function

ook like according to our picture of the
ssed by successive approximation; see Fig.
transition from scenario 2 to 3 is of course
nteract, they can redistribute the momenta
lefined momentum $x = \frac{1}{3}$ is washed out,
peaked around $x = \frac{1}{3}$. Data on $F_2^{ep}(x)$ at
ape of scenario 4 corresponding to Fig. 9.5.

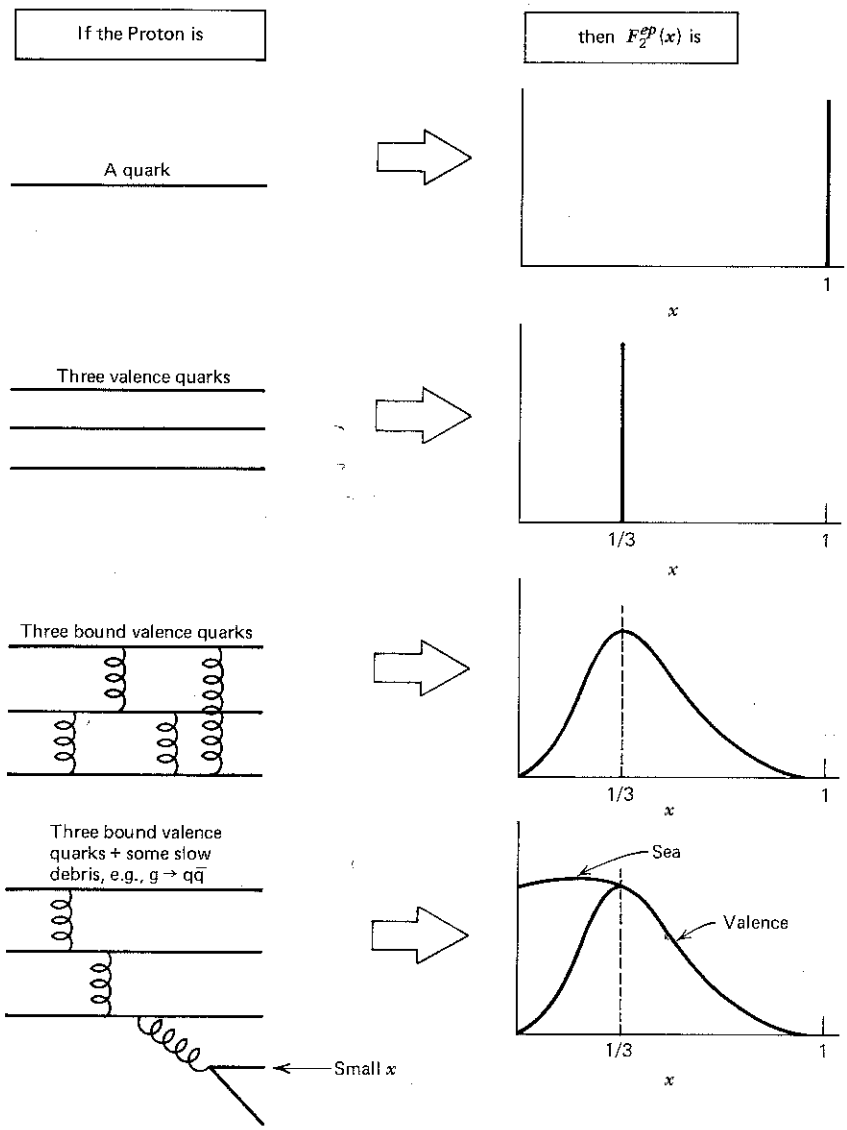

Fig. 9.7 The structure function pictured corresponding to different compositions assumed for the proton.

However, by subtracting eqs. (9.32),

$$\frac{1}{x}\left[F_2^{ep}(x) - F_2^{en}(x)\right] = \frac{1}{3}\left[u_v(x) - d_v(x)\right], \tag{9.36}$$

we can observe the valence quarks without their sea quark partners. The result should look like scenario 3 of Fig. 9.7 and should peak around $\frac{1}{3}$. It does, as can be seen in Fig. 9.8.

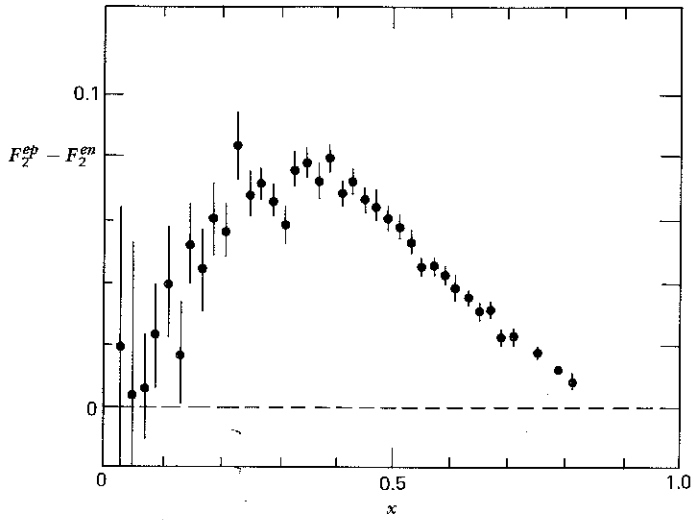

Fig. 9.8 The difference $F_2^{ep} - F_2^{en}$ as a function of x, as measured in deep inelastic scattering. Data are from the Stanford Linear Accelerator.

An alternative phenomenological approach is to parametrize all large Q^2 data on $F_2^{ep,\,en}(x)$ in terms of the valence and sea distributions and extract the quark structure functions at each x subject to the sum rules (9.31). The result of such an analysis is shown in Fig. 9.9. Fig. 9.9a shows the $\bar{q}$ distribution, which has been subjected also to assumption (9.30). We see how $u(x) = u_v(x) + u_s(x)$ approaches $\bar{u}(x)$ at small x as $xu_v(x) \to 0$. Figure 9.9b displays the general shape of the total valence and sea quark components, corresponding to scenarios 3 and 4 in Fig. 9.7. Note how slow the sea quarks are as compared to their valence partners.

9.4 Where Are the Gluons?

If we sum over the momenta of all the partons, we must reconstruct the total momentum p of the proton [see (9.8)],

$$\int_0^1 dx\,(xp)[u + \bar{u} + d + \bar{d} + s + \bar{s}] = p - p_g,$$

or, dividing by p,

$$\int_0^1 dx\,x(u + \bar{u} + d + \bar{d} + s + \bar{s}) = 1 - \varepsilon_g. \tag{9.37}$$

The momentum fraction $\varepsilon_g \equiv p_g/p$ carried by the gluons is not directly exposed

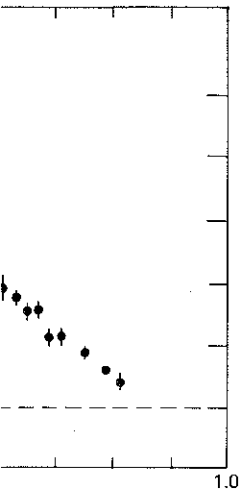

ction of x, as measured
n the Stanford Linear

to parametrize all large Q^2 data
tributions and extract the quark
ules (9.31). The result of such an
$\bar{q}$ distribution, which has been
how $u(x) = u_v(x) + u_s(x)$ ap-
.9b displays the general shape of
responding to scenarios 3 and 4
as compared to their valence

, we must reconstruct the total

$$+ \bar{s}] = p - p_g,$$

(9.37)

$$\bar{s}) = 1 - \varepsilon_g.$$

e gluons is not directly exposed

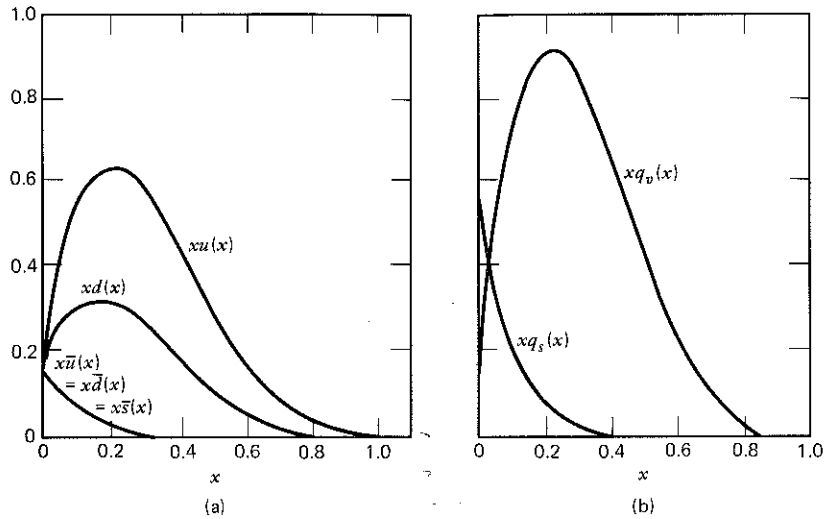

Fig. 9.9 The quark structure functions extracted from an analysis of deep inelastic scattering data. Figure (b) shows the total valence and sea quark contributions to the structure of the proton.

by the photon probe (since gluons carry no electric charge) and is therefore subtracted from the right-hand side. Integrating over the experimental data on $F_2^{ep,\,en}(x)$ gives us the following information:

$$\int dx\, F_2^{ep}(x) = \tfrac{4}{9}\varepsilon_u + \tfrac{1}{9}\varepsilon_d = 0.18,$$

$$\int dx\, F_2^{en}(x) = \tfrac{1}{9}\varepsilon_u + \tfrac{4}{9}\varepsilon_d = 0.12, \qquad (9.38)$$

where

$$\varepsilon_u \equiv \int_0^1 dx\, x(u + \bar{u})$$

is the momentum carried by u quarks and antiquarks, and similarly for ε_d. Equation (9.38) follows from (9.27) and (9.28) after neglecting the strange quarks which carry a small fraction of the nucleon's momentum. From (9.37), we have

$$\varepsilon_g \simeq 1 - \varepsilon_u - \varepsilon_d,$$

and on solving (9.38), we obtain

$$\varepsilon_u = 0.36, \qquad \varepsilon_d = 0.18, \qquad \varepsilon_g = 0.46. \qquad (9.39)$$

Hence, the gluons carry about 50% of the momentum, which was unaccounted for by the charged quarks.

In summary, an analysis of data on deep inelastic scattering of leptons by nucleons reveals the presence of point-like Dirac particles inside hadrons through Bjorken scaling. A study of the quantum numbers of these partons allows us to identify them with the quarks introduced in the study of the hadron spectrum in Chapter 2. The momentum distribution of the quarks forces us to the conclusion that a substantial fraction of the proton's momentum is carried by neutral partons, not by quarks. These are the gluons of QCD.